Model Predictive Control for Spacecraft Rendezvous and Docking: Strategies for Handling Constraints and Case Studies

Avishai Weiss, Morgan Baldwin, Richard Scott Erwin, and Ilya Kolmanovsky

***Abstract*— This paper presents a strategy and case studies of spacecraft relative motion guidance and control based on the application of linear quadratic model predictive control (MPC) with dynamically reconfigurable constraints. The controller is designed to transition between the MPC guidance during a spacecraft rendezvous phase and MPC guidance during a spacecraft docking phase, with each phase having distinct requirements, constraints, and sampling rates. Obstacle avoidance is considered in the rendezvous phase, while a line-of-sight cone constraint, bandwidth constraints on the spacecraft attitude control system, and exhaust plume direction constraints are addressed during the docking phase. The MPC controller is demonstrated in simulation studies using a nonlinear model of spacecraft orbital motion. The implementation uses estimates of spacecraft states derived from relative angle and range measurements, and is robust to estimator dynamics and measurement noise.**

***Index Terms*— Constraints, model predictive control, obstacle avoidance, rendezvous and docking, spacecraft control.**

I. Introduction

AUTONOMOUS spacecraft rendezvous and docking maneuvers are among the most important and difficult components of modern spacecraft missions [1]. Examples include transport vehicle approach and docking to the International Space Station, capture and recovery of tumbling satellites, and avoidance or flybys of space objects (e.g., debris). Traditionally, relative motion maneuvers are performed using *open-loop* planning techniques [2]. *Ad hoc* maneuver corrections may be employed to compensate for errors inherent in open-loop control. The literature on spacecraft rendezvous control is extensive and includes, for instance, [2]–[6], and the references therein.

Recently, more interest has been emerging in *closed-loop* maneuvering, especially for missions that involve formation flying or automated rendezvous, docking, and proximity operations. The robustness, fuel efficiency, speed, safety, and reliability of spacecraft relative motion maneuvers may be improved through the judicious application of feedback control.

With this motivation, in [7] and [8], an approach to perform relative motion maneuvers based on the application of linear quadratic model predictive control (MPC) and dynamically reconfigurable linear constraints was developed. This approach enables fuel efficient maneuvers that, in real time, can be replanned to account for unmeasured disturbances, changing target conditions or objectives, and time-varying path constraints, such as the presence of obstacles or debris. The MPC controller uses a linearized relative motion model and linear constraints that are generated online to compute the optimal control sequence over a finite horizon; it then applies the first element of this sequence to the spacecraft and repeats the process at the next sampling instant. For maneuvers confined to the orbital plane, Park *et al.* [7] and Di Cairano *et al.* [8] demonstrated the capability to approach both a nonrotating and rotating, or tumbling, platform, while avoiding an obstacle along the spacecraft's path. In addition, robustness to unmeasured disturbances through the mechanism of systematic MPC feedback corrections was demonstrated. Finally, it was shown that the linear quadratic MPC approach with dynamically reconfigurable constraints reduces to an on-line solution of a quadratic programming (QP) problem, which is computationally feasible on-board a spacecraft. Furthermore, if the spacecraft approaches a nonrotating platform with a known line-of-sight (LoS) cone orientation, an explicit MPC approach that does not require on-board optimization can be used, and is based on storing an offline precomputed MPC law in the form of a piecewise affine control function (i.e., in the form of lookup tables and if-then-else conditions). The main limitation of [7] and [8] is that relative motion maneuvers are confined to the orbital plane of the target spacecraft.

Several other variants of the MPC framework for relative motion control have been proposed in the literature. The approach employed in [3] and [9] uses a variable length horizon and requires the solution of a mixed-integer linear program at every control step. An application of MPC to spacecraft guidance in proximity of a space station is considered in [10], where an unconstrained MPC is proposed for guidance to the neighborhood of the space station, while the LoS between the station and the spacecraft sensors is maintained by a constrained spacecraft attitude controller and a control allocation scheme to operate the thrusters. In a similar context, a receding horizon controller that uses the solutions

Manuscript received March 10, 2014; revised July 22, 2014; accepted November 8, 2014. Date of publication January 16, 2015; date of current version June 12, 2015. Manuscript received in final form November 26, 2014. This work was supported in part by the American Society for Engineering Education through the Air Force Summer Faculty Fellow Program and in part by the National Science Foundation through the University of Michigan, Ann Arbor, MI, USA, under Award 1130160. Recommended by Associate Editor M. Mattei.

A. Weiss was with the Department of Aerospace Engineering, University of Michigan, Ann Arbor, MI 48109 USA (e-mail: avishai@umich.edu). This research was not sponsored by Mitsubishi Electric or its subsidiaries.

M. Baldwin and R. S. Erwin are with the Space Vehicle Directorate, Air Force Research Laboratory, Albuquerque, NM 87116 USA (e-mail: afrl.rvsv@kirtland.af.mil).

I. Kolmanovsky is with the Department of Aerospace Engineering, University of Michigan, Ann Arbor, MI 48109 USA (e-mail: ilya@umich.edu).

Color versions of one or more of the figures in this paper are available online at http://ieeexplore.ieee.org.

Digital Object Identifier 10.1109/TCST.2014.2379639

of nonconvex quadratically constrained QP has been proposed in [11] for passively safe proximity operations, where a statistical model of the uncertainty is used for improving robustness with respect to position uncertainty.

In this paper, we extend the approach developed in [7] and [8]. This includes the treatment of 3-D relative motion maneuvers with 3-D LoS cone constraints, the use of an MPC controller to prescribe Δv impulsive velocity changes rather than piecewise constant thrust profiles as in [7] and [8], and the demonstration of the ability to transition between the MPC guidance in the spacecraft rendezvous phase and MPC guidance in the spacecraft docking phase, with requirements, constraints, and sampling rates specific to each phase. To avoid the need for a long MPC control horizon or long sampling periods in the rendezvous phase, a reference governor-like approach motivated by [12] and [13], where the desired equilibrium set point is replaced by a virtual set point, is employed. In addition, bandwidth constraints on the spacecraft attitude control system are treated, while thrust direction constraints are handled by introducing an appropriate penalty term in the cost function and a relative-distance-dependent constraint on the thrust vector. In addition, 3-D obstacle avoidance is demonstrated using a dynamically reconfigurable hyperplane constraint. The obstacle is assumed to be changing in size, which corresponds to changes in the uncertainty estimates of its location. The MPC controller is validated on a full nonlinear model of spacecraft orbital motion, and it is demonstrated that the MPC feedback can be implemented with only measurements of relative angles and range. To accomplish the latter, an extended Kalman filter (EKF) is utilized to provide state estimates for the MPC controller. The simulation results based on a set of parameters representative of a small spacecraft with limited thrust capability are shown. As compared with [14], this paper additionally treats obstacle avoidance maneuvering, which is a particularly challenging and nonconvex problem, and overall contains more details, case studies, interpretations, and discussion.

The details of this MPC approach differ from [15] in that our approach is based on a QP [versus linear programming (LP) in [15]], uses a reference governor style formulation of MPC cost for the rendezvous phase, explicitly handles LoS cone and obstacle avoidance constraints, and accounts for the capability of the attitude control system with an attitude penalty in the cost. The use of a QP (rather than LP) formulation is exploited due to its close connection to LQR control, and that local stability can be ensured based on selecting the terminal penalty as the solution to a Riccati equation (Remark 1). QP solutions can provide smoother control actions and easier tuning [16] and, in the case of a single thruster spacecraft configuration, there is no generic advantage to using LP formulation in penalizing the fuel consumption. Finally, while the focus of this paper is on maneuvering relative to a location on a circular orbit due to a class of missions of interest, the extension to the case of elliptic orbits (treated in [15]) is feasible by employing orbit position-dependent linearization for the prediction model. The results of our paper, obtained independently of [15], confirm the capability of MPC in being an effective technology for relative motion maneuvering. In what follows, we present the model, our approach to MPC design, case studies, and concluding remarks.

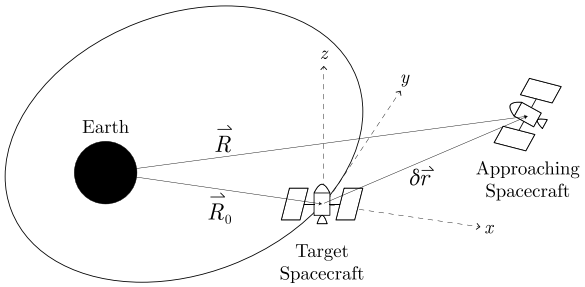

Fig. 1. Hill's frame.

II. Model

In traditional relative motion problems, an approaching spacecraft is maneuvered close to a target spacecraft in a nominal orbit. The target spacecraft is assumed to be at the origin of Hill's frame [17] (Fig. 1).

The relative position vector of the spacecraft with respect to a target location on an orbit is expressed as

$$\delta\vec{r} = x\hat{i} + y\hat{j} + z\hat{k}$$

where x, y, and z are the components of the position vector of the spacecraft relative to the target location and $\hat{i}$, $\hat{j}$, and $\hat{k}$ are the unit vectors of the Hill's frame. The Hill's frame has its x-axis along the orbital radius, y-axis orthogonal to the x-axis and in the orbital plane, and z-axis orthogonal to the orbital plane.

The position vector of the spacecraft with respect to the center of the earth is given by $\vec{R} = \vec{R}_0 + \delta\vec{r}$, where $\vec{R}_0$ is the nominal orbital position vector. The nonlinear equation of motion for the spacecraft (relative to an inertial frame) is given by

$$\ddot{\vec{R}} = -\mu\frac{\vec{R}}{R^3} + \frac{1}{m_c}\vec{F} \tag{1}$$

where $\vec{F}$ is the vector of external forces applied to the spacecraft, $R = |\vec{R}|$, m_c is the mass of the spacecraft, and μ is the gravitational constant.

For $\delta r \ll R$, the linearized Clohessy–Wiltshire–Hill (CWH) equations [18] approximate the motion of the spacecraft relative to a target or a nominal location on a circular orbit as

$$\begin{aligned} \ddot{x} - 3n^2x - 2n\dot{y} &= \frac{F_x}{m_c} \\ \ddot{y} + 2n\dot{x} &= \frac{F_y}{m_c} \\ \ddot{z} + n^2z &= \frac{F_z}{m_c} \end{aligned} \tag{2}$$

where F_x, F_y, and F_z are the components of the external force vector (excluding gravity) acting on the spacecraft, such as propulsive forces, air drag, and solar radiation pressure. $n = (\mu/R_0^3)^{1/2}$ denotes the mean motion parameter of the nominal orbit, and R_0 is the nominal orbital radius of the

target vehicle. The linearized dynamics account for differences in gravity between the spacecraft and nominal orbital location, and for relative motion effects. Note that circular orbit equilibria are open-loop stable in radius and unstable in phase.

The continuous-time model (2) is converted to discrete time for use as a prediction model in MPC. As is commonly done [4], the effects of thrust are modeled as impulsive changes Δv_k in relative velocity of the approaching spacecraft at time instant t_k. Assuming a period of ΔTs between the impulsive velocity changes, the discrete-time model is given by

$$X_{k+1} = AX_k + BU_k \tag{3}$$

where $X_k = [x_k,\ y_k,\ z_k,\ \dot{x}_k,\ \dot{y}_k, \dot{z}_k]^T$ is the state at time step $k \in Z^+$, $U_k = \Delta v_k$ is the control vector at the time step $k \in Z^+$, A is state transition matrix over a time period ΔT of the continuous-time linear system (2), and $B = A\bar{B}$, where the constant matrix $\bar{B}$ maps the velocity change Δv_k to the full state change

$$\bar{B} = \begin{bmatrix} 0_{3\times 3} \\ I_{3\times 3} \end{bmatrix}.$$

Thus, the discrete-time prediction model is obtained by propagating the change in state due to a velocity change induced by the thruster over a period of time ΔT of the continuous dynamics.

III. Model Predictive Controller

MPC represents an attractive framework to deal with the multitude of state and control constraints described below in the spacecraft relative motion problems. MPC generates control actions by applying a moving horizon trajectory optimization to predictions based on a system model subject to pointwise-in-time state and control constraints [19], [20]. The control is periodically recomputed with the current state estimate as an initial condition, thereby providing a feedback action that improves robustness to uncertainties and disturbances. A special formulation of the MPC optimization problem, where a rendezvous phase is separated from a docking phase, is necessary to avoid a long control horizon and solving a highly complex online optimization problem. For instance, longer sampling periods are introduced in the rendezvous phase, when the approaching spacecraft is further away from the target, versus the docking phase, when the approaching spacecraft is closer to the target. Various other steps need to be taken to convert the maneuver requirements into an MPC problem formulation that can be handled efficiently by MPC solvers. In particular, and as in the planar case [7], [8], we seek formulations that can be treated by QP solvers and have low computation overhead.

A. Penalties and Constraints

During rendezvous and docking, the space vehicle must adhere to various constraints [7], [8], subsequently discussed, while executing the maneuver. While the developments are easily generalizable, we make our problem formulation specific to a spacecraft that performs a rendezvous and docking maneuver with the target at the origin of Hill's frame from the $+y$-direction in the docking phase. This is the so-called V-bar approach.

Depending on the portion of the relative motion maneuver being completed, different constraints must be addressed pertaining to the vehicle and the path it takes. For example, a space vehicle cannot produce limitless thrust in any direction; therefore, Δv magnitude and direction must be limited during both rendezvous and docking. However, the orientation of the vehicle is only constrained during the docking phase to avoid hitting the target with exhaust plumes, and does not play a major role in the rendezvous phase. Certain constraints may be treated as soft to enhance solution feasibility, and as such we implement them as penalties in the MPC cost.

We consider the discrete-time spacecraft model (3) with the velocity impulses $U_k = \Delta v_k = \Delta[\dot{x}_k\ \dot{y}_k\ \dot{z}_k]^T$ as the control signals. Impulse-based control of spacecraft is often assumed in relative motion problems [4]. Maximum Δv constraints

$$|U_k|_\infty \leq u_{\max} \tag{4}$$

are implemented during both rendezvous and docking to adhere to the finite thrusting capability of the vehicle, where $u_{\max} = 10$ m/s. As in [8], even for a single thruster spacecraft configuration, we use ∞-norm bounds rather than two-norm bounds for computational reasons: The problem remains a QP, while conservatism is avoided by setting $u_{\max}$ in (4) as the ∞-norm bound and directionally preserving scaling to satisfy the original two-norm constraint. Alternatively, a polyhedral approximation of a two-norm bound can be employed.

During the docking phase, thrust direction limits are imposed so that the spacecraft does not fire its thrusters into the target. This requirement is treated by imposing a time-varying control constraint. For example, considering an in-orbital track target with an approach from $+y$, this constraint is given by

$$\Delta \dot{y}_k \leq \mu e^{-\beta k}, \quad \mu > 0,\ \beta > 0 \tag{5}$$

that is, the Δv component in the positive y-direction is progressively constrained as the spacecraft approaches the target. We consider a spacecraft configuration that includes only one thruster. To enable an attitude controller to keep up with commanded thrust direction changes, we augment the MPC cost function with a term

$$\sum_{k=0}^{N} (U_k - U_{k-1})^T R^{\text{attitude}} (U_k - U_{k-1}) \tag{6}$$

where $R^{\text{attitude}} = (R^{\text{attitude}})^T \succ 0$. This term penalizes the rate of thrust vector changes and we found it to be effective in dealing with attitude controller bandwidth and capability limits. R^{attitude} is made to be a function of control magnitude so that it retains the same relative weight in the cost function irrespective of the magnitude of U_k. The quadratic form of (6) facilitates the application of QP-based MPC solvers.

Several path constraints are implemented to ensure a safe trajectory for the vehicle. During the docking phase, the target vehicle's sensors constrain the approaching space vehicle. We implement this constraint using an LoS cone that emanates from the docking port [9]. LoS cone constraints in three

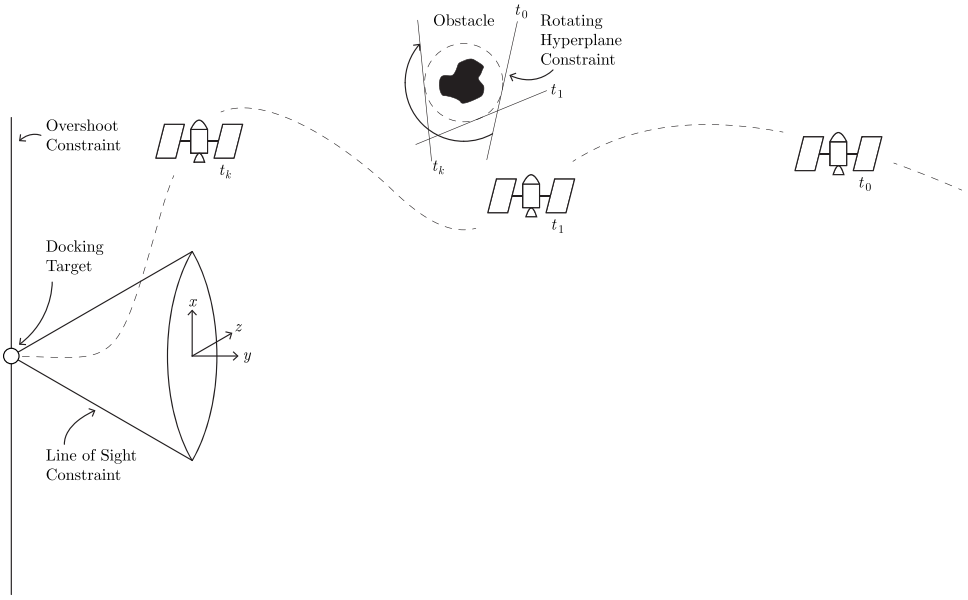

Fig. 2. Schematic of a spacecraft docking maneuver subject to LoS, overshoot, and obstacle avoidance constraints. The spacecraft position and the position of the rotating hyperplane are shown at discrete time instants t_0, t_1, and t_k.

dimensions are quadratic. Since we subsequently formulate the MPC problem as a quadratic program with affine constraints, we reformulate these constraints using an inner polyhedral approximation given by

$$A_{\text{cone}} X \leq b_{\text{cone}}. \tag{7}$$

In our numerical experiments, we use an approximation based on 10 vertices. We treat the LoS constraint as soft by imposing a penalty for deviations outside the LoS cone and augmenting this penalty to the MPC cost function. This cost is given by

$$\sum_{k=1}^{N} \lambda \mathbf{1}^T (A_{\text{cone}} X_k - b_{\text{cone}})_+ \tag{8}$$

where $(\cdot)_+$ denotes the positive part ($x_+ = x$ if $x > 0$ and 0 otherwise; applied componentwise), and λ is the weight. To avoid missing an in-track target, an overshoot constraint

$$y_k \geq 0 \tag{9}$$

is implemented. Constraints used in other docking approaches may be different but will have similar functional form.

Obstacle avoidance is a nonconvex problem with several possible formulations (e.g., mixed integer programming [21]). For this paper, as limited processing power is a driving factor, obstacle avoidance was addressed using linear dynamically reconfigurable constraints. Generalizing the approach in [8], a hyperplane is chosen to separate the obstacle from the space vehicle. The constraint is given by

$$n_k^T X_{\text{p},k} \geq n_k^T r_{\text{c},k} \tag{10}$$

where n_k is the normal vector to the hyperplane, $r_{\text{c},k}$ is a point on the boundary of the uncertainty ellipsoid associated with overbounding the obstacle, and $X_{\text{p},k}$ is the position of the vehicle at time step k. The hyperplane is rotated with a preselected rotation rate over the length of the maneuver by varying n_k and $r_{\text{c},k}$ so that the hyperplane normal guides the target spacecraft around the obstacle. The avoidance constraint (10) is capable of handling a growing or uncertain obstacle by manipulating $r_{\text{c},k}$. Note that the hyperplane rotation direction is dictated as a part of the problem formulation.

Fig. 2[1] shows a schematic of a docking maneuver subject to the discussed constraints.

B. MPC Problem Formulation

Using linearized equations of motion, linear equality and inequality constraints, and quadratic costs on the states and control actions, the MPC problem may be formulated as a QP problem. QPs can be solved using any number of generic solvers (for instance, MATLABs quadprog, and Parallel Quadratic Programming (PQP) [22]). Alternatively, using multiparametric programming, an explicit MPC approach that does not require on-board optimization may be used [23]. The downside of explicit solutions is that they are not straightforward to apply when dynamics or constraints are time varying, they may not scale well to large problems, and the execution times of lookup tables and logic may be longer than simply solving the QP numerically.

In this paper, we solve the QP in real time using CVXGEN, which generates efficient custom primal-dual interior-point solvers based on high-level problem descriptions [24]. Unlike the generic solvers, which solve single problem instances, CVXGEN accepts high-level descriptions of QP families and turns them into highly efficient flat, library-free C code that solve many problem instances. This strategy allows CVXGEN to exploit the structure (sparsity) of the specific QP family for fast run-time execution. This is useful in an MPC framework where the QP has a structure and is repeatedly solved at each sampling instant. The generated code does not branch, which allows for predictable run times, and is orders of magnitude faster than generic solvers [24], both highly desirable features

[1]The authors wish to thank Y. Weiss for generating Figs. 1 and 2.

for embedded applications with limited processing power such as on-board a spacecraft. The CVXGEN generated custom solver can handle time-varying dynamics and constraints. For instance, it is applicable to maneuvers on elliptic orbits [25].

Based on the practical considerations, the problem is separated into distinct rendezvous and docking phases. In the rendezvous phase, the spacecraft is a significant distance away from the target. A sampling period of 120 s is used and a Δv magnitude constraint is enforced. Since the thrust of the spacecraft is limited, to avoid the need for a long control horizon, a reference governor-like approach is introduced. In this approach, motivated by [12] and [13], the state set point, X_s is incorporated into the MPC problem formulation. The MPC controller adjusts this virtual set point, X_s, toward the actual set point (which is the origin in the rendezvous phase) because of the addition of the quadratic penalty $X_s^{\mathrm{T}} P X_s$ to the cost. We found that a reference governor is very useful to attain closed-loop stability and enlarge the domain of attraction when the prediction horizon is relatively short, as it avoids aggressive initial thrust from which the spacecraft is not able to recover. The rendezvous phase QP is given by

$$\begin{aligned}
\min\ & \sum_{k=0}^{N-1} (X_k - X_{\mathrm{s}})^T Q (X_k - X_{\mathrm{s}}) + X_{\mathrm{s}}^T P X_{\mathrm{s}} \\
& + \sum_{k=0}^{N-1} (U_k - U_{\mathrm{s}})^T R (U_k - U_{\mathrm{s}}) \\
& + (X_N - X_{\mathrm{s}})^T Q^{\mathrm{final}} (X_N - X_{\mathrm{s}}) \\
\text{s.t. } & X_{k+1} = A X_k + B U_k \\
& X_{\mathrm{s}} = A X_{\mathrm{s}} + B U_{\mathrm{s}} \\
& |U_k|_\infty \le u_{\max} \\
& n_k^T r_{c,k} - n_k^T X_{\mathrm{p},k} \le 0
\end{aligned} \tag{11}$$

where N is the control and prediction horizon, X_k and U_k are the state and control variables to be determined, X_{s} and U_{s} are the forced equilibrium state and control to be determined, Q and R are the specified weighting matrices, P is the weighting on the forced equilibrium states, and Q^{final} is the terminal state weighting matrix determined from the solution of the Riccati equation for the unconstrained infinite horizon problem. The equality constraint $X_{k+1} = AX_k + BU_k$ follows from the discrete CWH model (3), and $|U_k|_\infty \le u_{\max}$ is the maximum Δv constraint (4). If obstacle avoidance is not a part of the problem formulation, the constraint $n_k^T r_{c,k} - n_k^T X_k \le 0$ is omitted.

When the approaching spacecraft enters a specified box around the target, the docking phase begins. During this phase, the reference governor type action is removed as it is no longer necessary; the origin, that is the true desired equilibrium can be reached over the optimization horizon under the problem constraints. The sampling period is reduced to 20 s to facilitate faster control updates. An LoS cone constraint is imposed and is treated as soft via a polyhedral cost penalty (8). A thrust direction constraint (5) and an in-track target overshoot constraint (9) are also imposed. In addition, the rotation that the approaching spacecraft must perform between thrust impulses is approximately penalized by imposing a cost on change in control (6). The docking phase QP for constraints that are configured for an in-track V-bar approach, is given by

$$\begin{aligned}
\min\ & \sum_{k=0}^{N-1} X_k^T Q X_k + \sum_{k=0}^{N-1} U_k^T R U_k + X_N^T Q^{\mathrm{final}} X_N \\
& + \sum_{k=1}^{N} \lambda \mathbf{1}^T (A_{\mathrm{cone}} X_k - b_{\mathrm{cone}})_+ \\
& + \sum_{k=0}^{N} (U_k - U_{k-1})^T R^{\mathrm{attitude}} (U_k - U_{k-1}) \\
\text{s.t. } & X_{k+1} = A X_k + B U_k \\
& |U_k|_\infty \le u_{\max} \\
& \Delta \dot{y}_k \le \mu e^{-\beta k} \\
& y_k \ge 0
\end{aligned} \tag{12}$$

where X_k and U_k are the state and control variables to be determined, Q and R are the weighting matrices, Q^{final} is the terminal state weighting matrix determined from the solution of the Riccati equation, and U_{-1} is given from the previous step. The LoS cone and rotation rate constraints are implemented as soft constraints in the cost function using A_{cone} and b_{cone} for LoS and the weighting matrix R^{attitude} for the rotation rate. The equality constraint and the thrust constraint are the same as the rendezvous phase.

Remark 1: Consistent with the standard MPC approach (see [8], where the 2-D case is considered), we rely on inherent robustness of MPC to provide strong feedback and compensate for uncertainties, and, as in [8], we employ a terminal penalty matrix Q^{final} based on the solution to the LQR Riccati equation to achieve local stability near the target equilibrium. To formally take advantage of this approach, we slightly relax the constraints in our implementation so that they are inactive at the target equilibrium [e.g., (9) is replaced by $y_k \ge -\epsilon$, $\epsilon > 0$]. While we assure local stability, estimates of the domain of attraction for the closed-loop nonlinear system can be obtained via simulations [26]. In [26], we also considered an approach to guarantee stability in the docking phase via terminal state constraints. As this led to increased fuel consumption and may actually reduce the closed-loop domain of attraction, we did not include terminal set constraints in (12). With most constraints treated as soft, we note that recursive feasibility of (11) and (12) is guaranteed by relaxing hard constraints with slack variables. Uncertainty can be handled upfront exploiting robust MPC approaches [27], but this may lead to conservative and computationally expensive solutions.

C. Implementation Using State Estimates

The MPC controller may be implemented using only the output measurements of relative range and angles, given by

$$\begin{aligned}
Y_1 &= \sqrt{x^2 + y^2 + z^2} + \nu_1 \\
Y_2 &= \mathrm{atan2}\,(x, y) + \nu_2 \\
Y_3 &= \mathrm{atan2}\left(z, \sqrt{x^2 + y^2}\right) + \nu_3
\end{aligned} \tag{13}$$

where x, y, and z are the relative x-, y-, and z-position, respectively, atan2 denotes the four-quadrant arctangent, and

ν_1, ν_2, and ν_3 are the measurement noise in each output channel. An EKF based on the CWH equations is used to estimate the spacecraft states given the measurements [28]. The output measurement equations are nonlinear and hence the convergence of the EKF estimates is only expected when the state estimate is initialized sufficiently close to the true state.

IV. Case Studies

In Sections IV-A and IV-B, we discuss the case studies that highlight various unique features of our MPC solution. Section IV-C provides three complete rendezvous and docking maneuvers using only relative range and angle measurements.

A. Attitude Control Penalty

The effects of including the attitude control penalty $R^{\text{attitude}} \neq 0$ are apparent in Fig. 3. The average angle between consecutive velocity changes is smaller when including the penalty, reducing the effort of the attitude control system to change the orientation before the next thrust event.

B. Obstacle Avoidance

Fig. 4 shows the effect of hyperplane rotation rate on maneuvers for a growing obstacle. The obstacle may represent the uncertainty ellipsoid that is obtained from the error covariance matrix of the estimated obstacle position and size. The growing obstacle reflects the increasing amount of uncertainty about its relative position.

C. Rendezvous and Docking Maneuvers

Three complete maneuvers are now considered. They are patterned after typical approach and docking scenarios, and provide a good illustration of MPC controller capability and closed-loop trajectories.

- *Case 1:* A phasing maneuver with the approaching spacecraft in the same orbit but at a different true anomaly than the target. The LoS cone is oriented along the orbital track. This maneuver represents a V-bar docking with initial spacecraft position along V-bar. The initial position is $[0.63\ 10\ 0]^T$ km, and initial velocity is $[0\ 0\ 0]^T$ km/s.
- *Case 2:* The approaching spacecraft is in a lower orbit than the target. The LoS cone is positioned for V-bar docking. This maneuver represents a V-bar docking scenario with an initial spacecraft position along R-bar. The initial position is $[-2\ 0.126\ 0]^T$ km, and initial velocity is $[0\ 0\ 0]^T$ km/s.
- *Case 3:* Same as Case 2 but with the LoS cone positioned for R-bar docking, i.e., oriented along the radial line.

The control horizon and the prediction horizon N are fixed at 30 steps. The sampling period in the rendezvous phase is 2 min and is 20 s in the docking phase. The switch between the rendezvous and docking phases occurs when the estimated spacecraft position enters a 2-km box around the target. The spacecraft is in a nominal circular orbit at an altitude of 850 km above the earth. The fuel expenditure for all cases is summarized in Table I. The results of these case studies are now summarized individually.

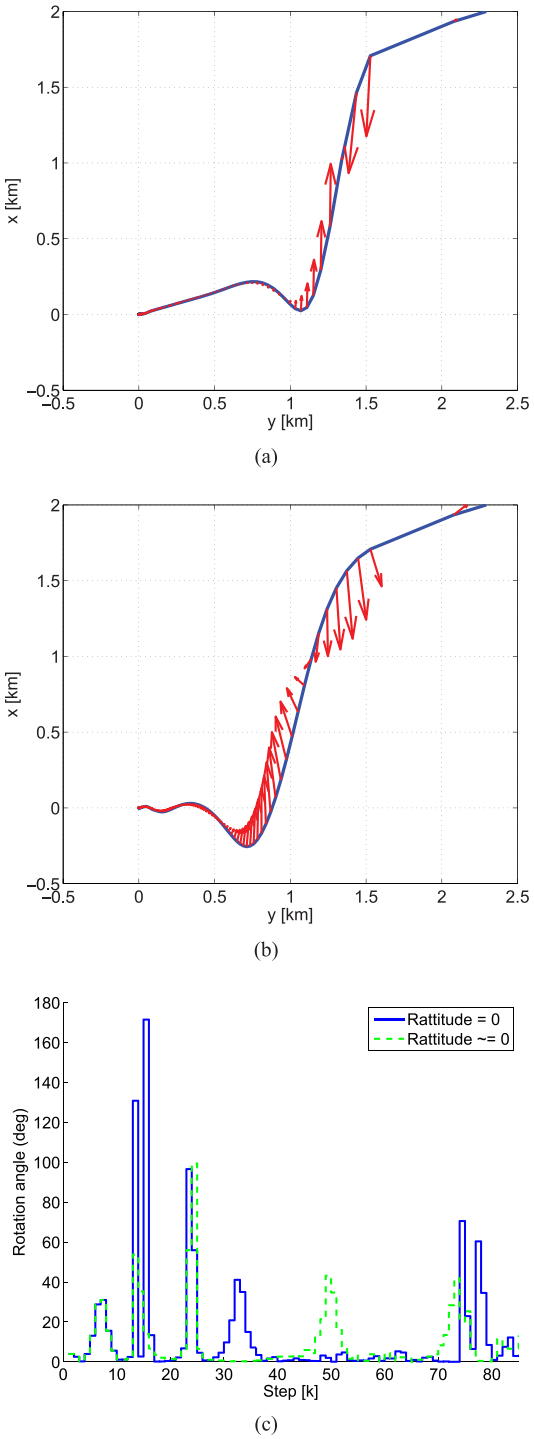

Fig. 3. Spacecraft trajectory on xy plane. Arrows indicate the direction and scaled magnitude of Δv's induced by thrusting. (a) With $R^{\text{attitude}} > 0$. (b) With $R^{\text{attitude}} = 0$. (c) Comparison of the angles between the two consecutive velocity changes for the cases (a) and (b).

TABLE I
TOTAL Δv FOR ALL MANEUVERS

Test case	1			2	3
	No obstacle	Clockwise Hyperplane Rotation	Counterclockwise Hyperplane Rotation		
Total Δv	.0366 km/s	.0354 km/s	.0410 km/s	.0073 km/s	.0145 km/s

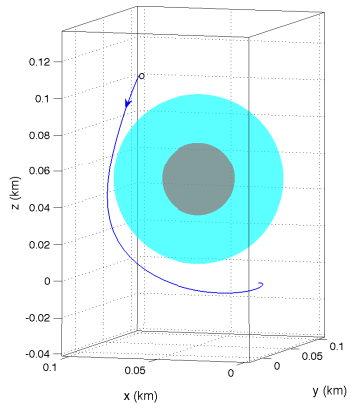

(a)

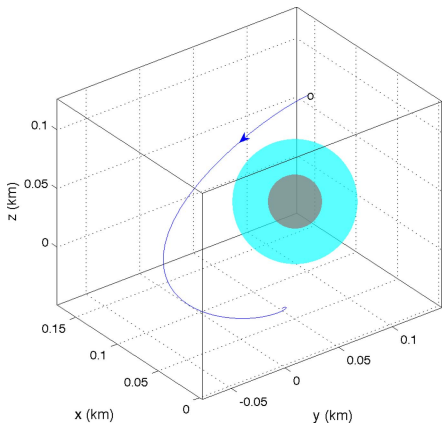

(b)

Fig. 4. Obstacle avoidance maneuvers using a rotating hyperplane constraint for two different rotation rates. The obstacle is growing, reflecting increasing levels of uncertainty. (a) Faster rotation rate. (b) Slower rotation rate.

1) Case 1 *(V-Bar Docking With Initial Spacecraft Position Along V-Bar):* The simulated MPC maneuver trajectories for V-bar docking with an initial spacecraft position along V-bar are shown in Fig. 5. The simulation results are obtained based on the *nonlinear* relative motion model (1). The MPC controller uses an EKF with the linearized CWH model (3) for prediction to estimate the spacecraft states based on relative range and angle measurements. The initial estimated state is $[-0.5\ 7\ 1.0\ 0\ 0\ 0]^T$ km. The EKF estimates converge rapidly to the actual states. Note that the spacecraft motion is 3-D even though the starting position is in the orbital plane. The out of orbital plane motion is excited since there is a nonzero initial estimation error of the spacecraft position in the z-direction that the MPC controller is trying to correct. Once the docking phase is started, the LoS cone constraint is activated. The trajectory enters into the LoS cone and proceeds toward the origin while satisfying the constraint. Large velocity changes are applied initially and become smaller and more gradual as the spacecraft approaches the origin; control activity increases

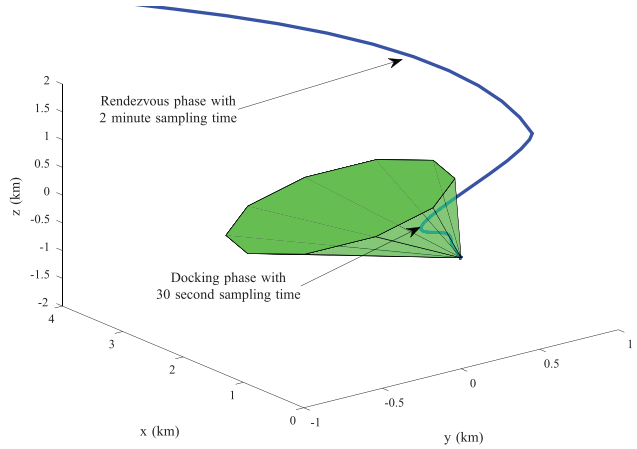

Fig. 5. Case 1. Trajectory in 3-D with rendezvous and docking phases and LoS cone constraints shown.

immediately after entering the docking phase and then decays. The time history of the velocity change direction indicates that the thrust in the direction of the target is minimized as the spacecraft approaches the target.

An obstacle is introduced during the rendezvous phase at $[1.3\ 5\ 0]^T$ km, which lies in the path of the unmodified trajectory. Fig. 6 shows the modified maneuver trajectories for a counterclockwise hyperplane rotation [Fig. 6(a)] and a clockwise hyperplane rotation [Fig. 6(b)]. The obstacle grows or becomes more uncertain as time progresses. The hyperplane constraints are not redundant as observed in Fig. 6(e) and (f), where the unmodified trajectory (dashed–dotted) violates the constraint. The hyperplane constraints are temporarily active for the modified trajectories (shown in solid). The counterclockwise rotation of the hyperplane forces the spacecraft radially outward, thus increasing the fuel expenditure (Table I). Note that fuel usage (measured in terms of total Δv) is assessed by summing up the two norms of velocity changes, i.e., $||\Delta v_k||$, over the simulated trajectory.

2) Case 2 *(V-Bar Docking With Initial Spacecraft Position Along R-Bar):* Fig. 7(a) shows a typical maneuver with the LoS cone constraint positioned for a V-bar approach [2]. The spacecraft, with initial position coordinates $[-2\ \ 0.126\ \ 0]^T$ and initial position coordinate estimates $[-2.8\ \ -0.01\ \ 0.1]^T$, starts the motion as in the R-bar approach. Once the docking phase is activated, the trajectory enters into the LoS cone positioned for a V-bar approach and proceeds toward the origin while satisfying the LoS cone constraint. The vehicle uses greater fuel at the beginning of the rendezvous phase to thrust the vehicle. The same increase in Δv demonstrated in the V-bar approach during the entry into the docking phase is evident in this case as well. This increase in Δv is necessary to meet the required constraints of the docking phase.

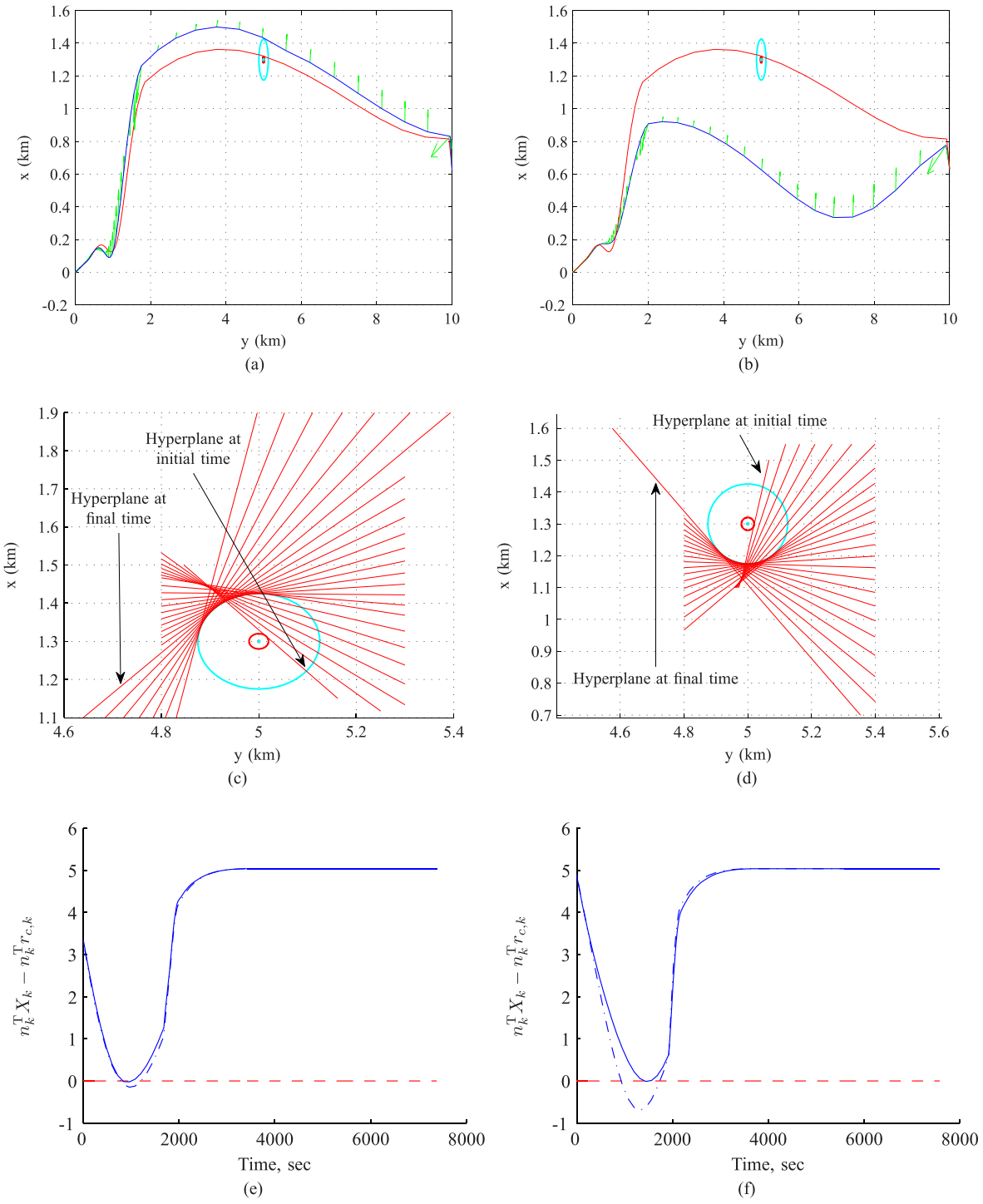

Fig. 6. Case 1. (a) and (b) Spacecraft trajectories in xy plane with and without obstacle avoidance. Initial position is $[0.63\ 10\ 0]^T$ km. An obstacle is located at $[1.3\ 5\ 0]^T$ km. (a) and (c) Counterclockwise rotation of the hyperplane. (b) and (d) Clockwise rotation of the hyperplane. (e) and (f) Time histories of hyperplane constraint with (solid) and without (dashed–dotted) obstacle avoidance for (e) counterclockwise and (f) clockwise hyperplane rotations. Negative values indicate a violation of the constraint.

3) Case 3 *(R-Bar Docking With Initial Spacecraft Position Along R-Bar):* Fig. 7(b) shows a maneuver similar to Case 2 but with the LoS cone constraint positioned for an R-bar approach. The behavior is qualitatively similar to the one in Fig. 7(a). The constraints and maneuver requirements are satisfied using the proposed MPC approach.

The above simulations were carried out on a 2.4-GHz Intel Core i5 processor. The custom CVXGEN solvers were compiled using GCC 4.2 with the level 1 optimization flag enabled, and run with default convergence tolerances. As CVXGEN treats both state and control variables over the horizon as independent, for the horizon of 30 steps, with a 6-D state vector and a 3-D control vector, the dimension of the underlying QP problems is 270. Average execution time of the rendezvous and docking phase QPs (11), (12) was 6.4 ms. Speedups may be

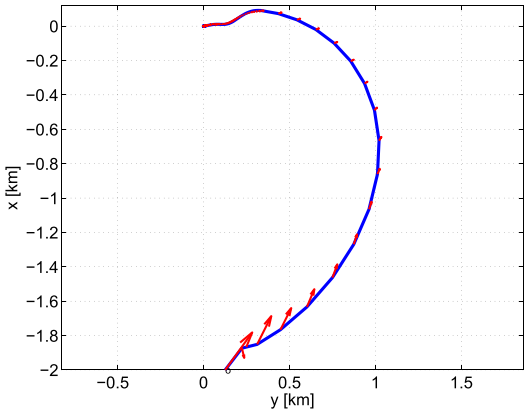

(a)

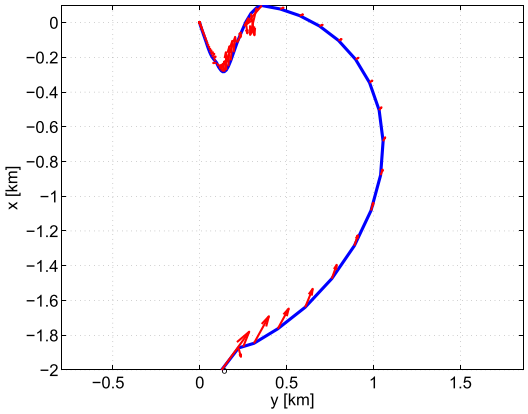

(b)

Fig. 7. (a) Case 2: spacecraft trajectory on xy plane with initial position $[-2,\ 0.126,\ 0]^T$ and the LoS cone pointed in the V-bar direction. (b) Case 3: spacecraft trajectory on xy plane with initial position $[-2,\ 0.126,\ 0]^T$ and the LoS cone pointed in the R-bar direction.

possible using updated compilers set with higher level optimization flags. A maximum time of 16.7 ms was recorded during a maneuver simulation when the spacecraft was near the obstacle, while a minimum time of 3.2 ms was representative of execution time during the docking phase. While kilohertz execution is attainable on commodity hardware, a 60-MHz processor that is 40 times slower would still have a maximum execution time of less than 1 s. Note that the sampling periods for the rendezvous and docking phases were 120 and 20 s, respectively, requiring that less than 5% of the spacecraft's CPU clock cycles be used for trajectory generation and control.

D. Total Δv Versus Time-to-Rendezvous

To study fuel usage (measured in terms of total Δv) relative to maneuver time, the relative weights Q and R are varied, generating a tradeoff curve for a phasing maneuver with V-bar docking. The initial position is $[0\ 2\ 0]^T$ km, and initial velocity is $[0\ 0\ 0]^T$ km/s. This curve, shown in Fig. 8, demonstrates that shorter maneuver times may be achieved at the cost of increased fuel consumption.

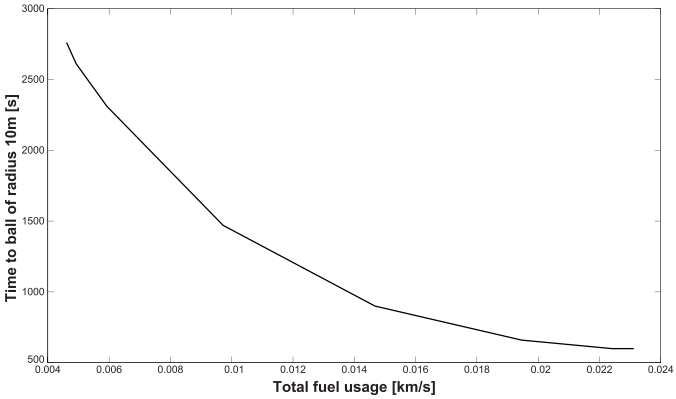

Fig. 8. Tradeoff curve demonstrating fuel usage of MPC controller with varying weight on fuel. Total fuel usage is determined by summing up the two-norm of the control over time.

V. Conclusion

In this paper, it was demonstrated through simulations on the full nonlinear model that the linear quadratic MPC controller with dynamically reconfigurable constraints can successfully complete a broad variety of 3-D relative motion maneuvers while satisfying path and control constraints and relying only on relative angles and range measurements. The approach presented only requires that a conventional quadratic program with linear inequality constraints be solved numerically.

References

[1] D. C. Woffinden and D. K. Geller, "Navigating the road to autonomous orbital rendezvous," *J. Spacecraft Rockets*, vol. 44, no. 4, pp. 898–909, 2007.

[2] W. Fehse, *Automated Rendezvous and Docking of Spacecraft* (Cambridge Aerospace). Cambridge, U.K.: Cambridge Univ. Press, 2003.

[3] L. Breger and J. P. How, "Safe trajectories for autonomous rendezvous of spacecraft," *J. Guid., Control, Dyn.*, vol. 31, no. 5, pp. 1478–1489, 2008.

[4] K. T. Alfriend, S. R. Vadali, P. Gurfil, J. P. How, and L. S. Breger, *Spacecraft Formation Flying* (Elsevier Astrodynamics). Oxford, U.K.: Elsevier, 2010.

[5] A. Miele, M. W. Weeks, and M. Circià, "Optimal trajectories for spacecraft rendezvous," *J. Optim. Theory Appl.*, vol. 132, no. 3, pp. 353–376, 2007.

[6] S. Nolet, E. Kong, and D. W. Miller, "Autonomous docking algorithm development and experimentation using the SPHERES testbed," *Proc. SPIE, Spacecraft Platforms Infrastruct.*, vol. 5419, pp. 1–15, Aug. 2004.

[7] H. Park, S. Di Cairano, and I. Kolmanovsky, "Linear quadratic model predicitve control approach to spacecraft rendezvous and docking," in *Proc. 21st AAS/AAIA Space Flight Mech. Meeting*, 2011, pp. 1–20.

[8] S. Di Cairano, H. Park, and I. Kolmanovsky, "Model predictive control approach for guidance of spacecraft rendezvous and proximity maneuvering," *Int. J. Robust Nonlinear Control*, vol. 22, no. 12, pp. 1398–1427, 2012.

[9] A. Richards and J. How, "Performance evaluation of rendezvous using model predictive control," in *Proc. AIAA Guid., Navigat., Control Conf.*, 2003, pp. 1–9.

[10] L. Singh, S. Bortolami, and L. A. Page, "Optimal guidance and thruster control in orbital approach and rendezvous for docking using model predictive control," in *Proc. AIAA Guid., Navigat., Control Conf.*, 2010, pp. 1–15.

[11] M. Holzinger, J. DiMatteo, J. Schwartz, and M. Milam, "Passively safe receding horizon control for satellite proximity operations," in *Proc. 47th IEEE Conf. Decision Control*, Dec. 2008, pp. 3433–3440.

[12] E. Gilbert and I. Kolmanovsky, "Nonlinear tracking control in the presence of state and control constraints: A generalized reference governor," *Automatica*, vol. 38, no. 12, pp. 2063–2073, 2002.

[13] A. Ferramosca, D. Limon, I. Alvarado, T. Alamo, and E. F. Camacho, "MPC for tracking with optimal closed-loop performance," *Automatica*, vol. 45, no. 8, pp. 1975–1978, 2009.

[14] A. Weiss, I. Kolmanovsky, M. Baldwin, and R. S. Erwin, "Model predictive control of three dimensional spacecraft relative motion," in *Proc. Amer. Control Conf. (ACC)*, Montreal, QC, Canada, Jun. 2012, pp. 173–178.

[15] E. N. Hartley, P. A. Trodden, A. G. Richards, and J. M. Maciejowski, "Model predictive control system design and implementation for spacecraft rendezvous," *Control Eng. Pract.*, vol. 20, no. 7, pp. 695–713, 2012.

[16] M. Barić, "Constrained control—Computations, performance and robustness," Ph.D. dissertation, Autom. Control Lab., ETH, Zürich, Switzerland, 2008.

[17] B. Wie, *Space Vehicle Dynamics and Control* (AIAA Education), 2nd ed. Reston, VA, USA: AIAA, 2008.

[18] W. H. Clohessy and R. S. Wiltshire, "Terminal guidance system for satellite rendezvous," *J. Aerosp. Sci.*, vol. 27, no. 9, pp. 653–658, 1960.

[19] S. S. Keerthi and E. G. Gilbert, "Optimal infinite-horizon feedback laws for a general class of constrained discrete-time systems: Stability and moving-horizon approximations," *J. Optim. Theory Appl.*, vol. 57, no. 2, pp. 265–293, 1988.

[20] E. F. Camacho, C. Bordons, E. F. Camacho, and C. Bordons, *Model Predictive Control*, vol. 303. Berlin, Germany: Springer-Verlag, 1999.

[21] A. Richards, T. Schouwenaars, J. P. How, and E. Feron, "Spacecraft trajectory planning with avoidance constraints using mixed-integer linear programming," *J. Guid., Control, Dyn.*, vol. 25, no. 4, pp. 755–764, Aug. 2002.

[22] M. Brand *et al.*, "A parallel quadratic programming algorithm for model predictive control," in *Proc. 18th World Congr. Int. Fed. Autom. Control (IFAC)*, vol. 18. 2011, pp. 1031–1039.

[23] P. Tøndel, T. A. Johansen, and A. Bemporad, "An algorithm for multi-parametric quadratic programming and explicit MPC solutions," *Automatica*, vol. 39, no. 3, pp. 489–497, 2003.

[24] J. Mattingley and S. Boyd, "CVXGEN: A code generator for embedded convex optimization," *Optim. Eng.*, vol. 13, no. 1, pp. 1–27, 2012.

[25] A. Weiss, I. Kolmanovsky, M. Baldwin, R. S. Erwin, and D. S. Bernstein, "Forward-integration Riccati-based feedback control for spacecraft rendezvous maneuvers on elliptic orbits," in *Proc. IEEE 51st Annu. Conf. Decision Control*, Maui, HI, USA, Dec. 2012, pp. 1752–1757.

[26] A. Weiss, "Predictive, adaptive, and time-varying control of spacecraft orbits and attitude," Ph.D. dissertation, Dept. Aerosp. Eng., Univ. Michigan, Ann Arbor, MI, USA, 2013.

[27] A. Bemporad and M. Morari, "Robust model predictive control: A survey," in *Robustness in Identification and Control*. London, U.K.: Springer-Verlag, 1999, pp. 207–226.

[28] A. Gelb, *Applied Optimal Estimation*. Cambridge, MA, USA: MIT Press, 1974.